EUROPHYSICS LETTERS 1 January 2006

Europhys. Lett., **73** (1), pp. 110–115 (2006)
DOI: 10.1209/epl/i2005-10360-3

Structural and optical properties of $BaTiO_3$ ultrathin films

Haizhong Guo[1], Lifeng Liu[1,2], Zhenghao Chen[1](*), Shuo Ding[1], Hubin Lu[1], Kui-juan Jin[1], Yueliang Zhou[1] and Bolin Cheng[1]

[1] *Beijing National Laboratory for Condensed Matter Physics, Institute of Physics Chinese Academy of Sciences - P.O. Box 603, Beijing 100080, PRC*
[2] *Department of Physics, Capital Normal University - Beijing 100037, PRC*

received 27 June 2005; accepted in final form 2 November 2005
published online 7 December 2005

PACS. 77.84.Dy – Niobates, titanates, tantalates, PZT ceramics, etc.
PACS. 78.30.-j – Infrared and Raman spectra.
PACS. 78.70.Ck – X-ray scattering.

Abstract. – Using laser molecular beam epitaxy technique, $BaTiO_3$ ultrathin films of 7, 12, 25, 750 monolayer (ML) thicknesses were obtained on MgO substrates. The effect of reducing the thickness of a $BaTiO_3$ film on its structural and optical properties was investigated by Raman scattering measurement, X-ray diffraction technique, and optical transmittance spectra. *In situ* reflection high-energy electron diffraction and X-ray diffraction observations have revealed that the $BaTiO_3$ films are epitaxially grown on MgO substrates from the initial stage without any other phase formation. Even in the sample of 7 ML, Raman scattering can reveal the structural information of the film. The $BaTiO_3$ ultrathin films have a highly *c*-axis–oriented tetragonal phase, and the formation of the perovskite phase is found in films as thin as 7 ML. An increase of the energy gap and the blue shifts of Raman modes are observed with reduction of the film thickness and the possible origin was analyzed.

Barium titanate ($BaTiO_3$) has comprehensive applications in pyroelectric detectors, non-volatile memory, electro-optic devices, and dynamic access memory because of its pyroelectricity, ferroelectricity, high dielectric constant and large electro-optic coefficients [1–4]. To meet the need of advanced integrated electronic devices, $BaTiO_3$ films deposited on substrates with small dimensions and perfect crystallinity morphology are required. Once deposited on the substrates, ferroelectric thin films can develop stress during the growth due to the lattice mismatch and the misfits in thermal expansion coefficients between the film and the substrate. The presence of stress can have significant effect on mechanical, electrical, and optical properties of ferroelectric thin films that can influence the reproducibility of the properties and reliability of the resulting devices [5–9].

The fabrication of $BaTiO_3$ thin films has been reported by techniques such as laser ablation [3], pulsed laser deposition [7], r.f. sputtering [8], metal organic chemical vapor deposition (MOCVD) [9], sol-gel processing [10], and laser molecular beam epitaxy (LMBE) [11]. Several kinds of single crystals such as $SrTiO_3$, MgO, and Pt have been used as substrates [3–11]. However, few papers in the literature reported on the fabrication of $BaTiO_3$ films as thin as

(*) E-mail: zhchen@aphy.iphy.ac.cn

a few ML. It is well known that the thinner is the film, the more boundary atoms exist in the film, and the larger strain has effect on the properties of the sample. Characterization techniques that provide information about the structure of ultrathin films are thus useful. Raman scattering is a powerful characterization technique, since the vibrational spectrum of the material is greatly influenced by disorder and residual stress: these cause changes in phonon frequencies and lifetimes, leading to the broadening of Raman peaks and to the breakdown of Raman selection rules [12]. Furthermore, the frequencies of phonons are sensitive to strains: positive (negative) frequency shifts are related to compressive (tensile) strain [13]. However, the Raman scattering intensities reported in the literature were too weak to reveal any structural information in ultrathin films. In the last few years, a number of groups have studied the structural distortions in ultrathin films [14–17]. To our knowledge, the effect of reducing the thickness of a BaTiO3 film on its optical properties is still rare in the literature.

In the present work, the highly *c*-axis–oriented single-crystal $BaTiO_3$ ultrathin films with different thicknesses were deposited by LMBE. Structure and optical properties were investigated by Raman measurement, X-ray diffraction (XRD) technique, and optical transmittance spectra. A variation with film thicknesses in the energy gap and Raman peaks was observed and the possible origin was analyzed.

By monitoring reflection high-energy electron diffraction (RHEED) intensity oscillations, a series of heteroepitaxial $BaTiO_3$ ultrathin films with 7, 12, 25, 750 ML thicknesses were deposited on single-crystal MgO substrates under an oxygen pressure of 8.0×10^{-1} Pa. Transparent and mirror-smooth films were realized by means of layer-by-layer growth. The beam of a Lambda Physik LEXTRA 200 excimer laser (308 nm, 20 ns, 2 Hz) was focused on a single-crystal $BaTiO_3$ target with an energy density of about $1\,J/cm^2$. During the deposition, the MgO substrates were heated up to 630 °C. To improve the quality of the films, we constructed an atomic oxygen source (AOS) and introduced it into the vacuum chamber of the LMBE system [18]. Oxygen passing through the AOS was partially ionized by a high-voltage discharge, resulting in the formation of atomic oxygen in the vacuum chamber. An electromagnetism-controlled valve was used to modulate the atomic oxygen flux. After deposition, the $BaTiO_3$ samples were annealed *in situ* for 30 minutes.

In situ RHEED patterns and intensity oscillations, and *ex situ* XRD were used to investigate the crystallinity and phase purity of the $BaTiO_3$ ultrathin films. The optical transmittances were measured at the wavelength range of 250–900 nm using a SpectraPro-500i spectrophotometer (Acton Research Corporation). Raman measurement for $BaTiO_3$ ultrathin films was performed in the backscattering geometry with a Jobin-Yvon T64000 triple Raman spectrometer. A 488 nm Ar^+ ion laser line was used for excitation. The spectrometer provided a wave number resolution of $0.5\,cm^{-1}$ and accuracy of $0.1\,cm^{-1}$. Two scattering geometries, parallel- and cross-polarizations, were used to obtain the polarized Raman spectra.

During the deposition of films, fine streak RHEED patterns and undamping RHEED intensity oscillations were observed. The results of RHEED observation indicate that the $BaTiO_3$ ultrathin films with smooth surfaces are two-dimensionally epitaxial growths on MgO substrates.

The XRD θ-2θ scan curves of the samples are shown in fig. 1. Except for $BaTiO_3$ (00l) and MgO (00l) peaks, there are other two diffraction peaks, one is MgO (200) K_β peak and the other (W peak) is due to the impurity of the X-ray beam induced by tungsten. There are no peaks from impurity phases or randomly oriented grains. Note that the XRD peaks became broader with the decrease of the film thicknesses. *In situ* RHEED and XRD observations have revealed that the $BaTiO_3$ films are epitaxially grown on MgO substrates from the initial stage without any other phase formation. Although the samples were strained by the epitaxial effect, the lattice parameters of c (0.405 nm) calculated from XRD results are almost the same

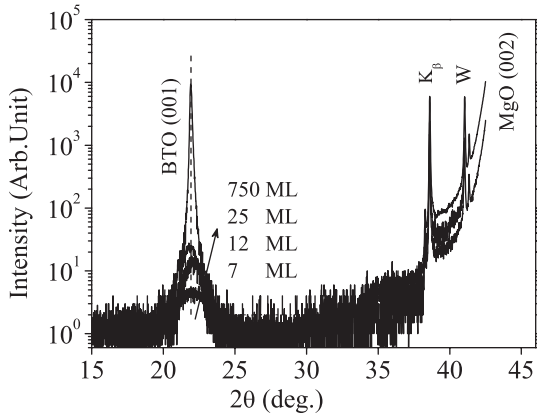

Fig. 1 – XRD θ-2θ scan curves of the $BaTiO_3$ ultrathin films with different thicknesses. The K_β peak is the MgO (200) K_β peak, and the W peak is due to the impurity of the X-ray beam induced by the tungsten.

as that of the $BaTiO_3$ bulk (0.404 nm), implying that the $BaTiO_3$ ultrathin films are highly c-axis oriented. Yoneda *et al.* [17] also observed that 50 ML thickness $BaTiO_3$ films on $SrTiO_3$ and MgO substrates had a highly c-axis–oriented tetragonal phase at room temperature, and the lattice parameter c of these films was very close to the bulk value of the tetragonal phase. It is worthy to note that our sample of 7 ML is at the tetragonal phase and is highly c-axis oriented, and the formation of the perovskite phase is found in the films as thin as 7 ML.

Figures 2(a) and (b) show the parallel- and cross-polarized Raman spectra of the samples with different thicknesses. The polarization direction of the incident laser is along the [100] direction of the MgO substrates. It should be noted that even in the sample of 7 ML, there exists a Raman signal, which can reveal the structural information. The parallel-polarized peaks around 890 and 970 cm^{-1}, and cross-polarized peaks at 800, 850, 890, and 1015 cm^{-1} are attributed to the second-order Raman peaks of the MgO substrate (indicated by * in

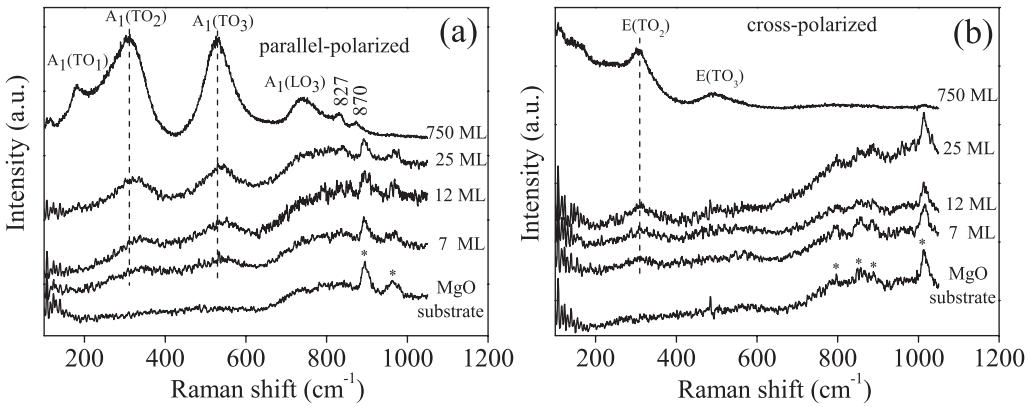

Fig. 2 – (a) Parallel- and (b) cross-polarized Raman spectra of the $BaTiO_3$ ultrathin films with different thicknesses and a single-crystal MgO substrate. The Raman peaks from the MgO substrate are indicated by *.

TABLE I – *Frequencies of the Raman peaks in* $BaTiO_3$ *ultrathin films with different thicknesses.*

Film thickness	7 ML	12 ML	25 ML	750 ML	Single crystal [20]
$E(TO_2)$ (cm^{-1})	305	305	305	305	305
$A_1(TO_2)$ (cm^{-1})	350	341	322	311	267
$A_1(TO_3)$ (cm^{-1})	550	542	538	529	512

fig. 2) [19]. Only A_1 and B_1 modes should be observable in the parallel-polarized spectra, while only the E modes should in the cross-polarized spectra. It is noticeable that the main typical features of the $BaTiO_3$ single crystal [20] have been clearly observed in the $BaTiO_3$ film with 750 ML thickness. In the parallel-polarized spectra (fig. 2(a)), the characteristic interference of the $A_1(TO_1)$ mode ($\sim 180\,cm^{-1}$) with a broad $A_1(TO_2)$ mode ($\sim 312\,cm^{-1}$) is due to the coupling between A_1 modes [21]. A third asymmetric $A_1(TO_3)$ mode appears at about $529\,cm^{-1}$ that also couples weakly with the $A_1(TO_2)$ mode. The $A_1(LO_3)$ mode is observed at $737\,cm^{-1}$. Additionally, two new high-frequency peaks at 827 and $870\,cm^{-1}$ are present, which maybe originate from the stress at the film-substrate interface [22]. In the cross-polarized spectra (fig. 2(b)), the $E(TO_2)$ mode ($\sim 305\,cm^{-1}$) and the $E(TO_3)$ mode ($\sim 489\,cm^{-1}$) have been observed in the $BaTiO_3$ thin film of 750 ML. However, because of their very weak intensity, the $A_1(LO_1)$ mode, the $A_1(LO_3)$ mode, and two new high-frequency peaks in the parallel-polarized spectra, and the $E(TO_3)$ mode in the cross-polarized spectra have not been observed in the $BaTiO_3$ ultrathin films with 7, 12, and 25 ML thicknesses. The $A_1(LO_1)$ mode ($\sim 727\,cm^{-1}$) and the $E(TO_2)$ mode ($\sim 305\,cm^{-1}$) are specific to the tetragonal phase of $BaTiO_3$ [18], and their appearances further confirm the tetragonal structure of the $BaTiO_3$ ultrathin films, which correspond to XRD measurements.

Notice that all the Raman peaks of the samples become broad and gradually lose their intensity with the decrease of the film thickness, indicating that there are more lattice deformation, more boundary atoms, and more disorder in thinner films. The peak at the $305\,cm^{-1}$ mode remains at the same frequency. The frequencies of $A_1(TO_2)$ and $A_1(TO_3)$ modes are appreciably higher than the corresponding phonon frequencies in the $BaTiO_3$ single crystal [18]. Table I shows the change of frequencies of Raman peaks with film thicknesses. The blue shifts are related to compressive stresses in the $BaTiO_3$ ultrathin films, which result from the differences of the lattice parameters and the thermal expansion coefficient between films and substrates [23]. Furthermore, the thinner the film, the more the Raman peaks shift to higher frequencies. This suggests that compressive stress is more pronounced in thinner films.

The optical transmittance spectra for the $BaTiO_3$ ultrathin films are shown in fig. 3. The oscillation in the transmittance spectra of the 750 ML thickness sample comes from the interference due to reflection from the top surface of the film and the interface between the film and substrate. The transmittance curves of the ultrathin films dropped off near 340 nm and the films show good transparency in the visible and near-infrared region. The absorption coefficient a is related to the band gap E_g as $(h\nu\alpha)^2 = B(h\nu - E_g)$, where $h\nu$ is the incident photon energy, and B is constant [24]. The graph of $(h\nu\alpha)^2$ *vs.* $h\nu$ is shown in fig. 4. By extrapolating the linear portion of the curves to intersect with the x-axis, the band gap energies were obtained for the ultrathin $BaTiO_3$ films. The values are 3.70, 3.77, 3.82, and 3.87 eV corresponding to the 750, 25, 12, and 7 ML $BaTiO_3$ ultrathin films, respectively. With the increase of thicknesses, the band gap of $BaTiO_3$ ultrathin films shifts to a lower energy and tends toward a value of 3.6 eV for bulk single crystal [24]. In other word, the thinner the film is, the greater the energy gap deviates from that of the bulk crystal. The variation of the lattice parameters, the boundary atoms, and strain may be the reasons for the variation of

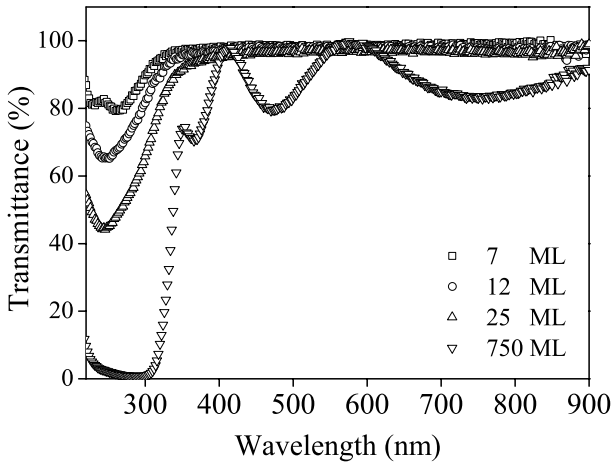

Fig. 3 – Optical transmission as a function of the wavelength of the $BaTiO_3$ ultrathin films with different thicknesses.

the energy gap with different thicknesses [10]. In our case, the variation of lattice parameters is not the main reason for the variation of the energy gap, since the c lattice parameters of these ultrathin films calculated from XRD results are almost the same. In our ultrathin films, the decrease of thicknesses is accompanied by the increases of the boundary atoms and the compressive stress, which is confirmed by Raman scattering measurement. The boundary atoms can cause a decrease of the widening of the lowest conduction band and the highest valence band, resulting in an increase of the energy gap in $BaTiO_3$ thin films. The thinner the film, the broader the energy gap.

In conclusion, $BaTiO_3$ ultrathin films with thicknesses in the range of 7 to 750 ML were prepared by LMBE. Optical transmittance and Raman spectra were analyzed to investigate the structural and optical properties of $BaTiO_3$ ultrathin films with different thicknesses. The results show that the films have a highly c-axis–oriented tetragonal phase, and the formation

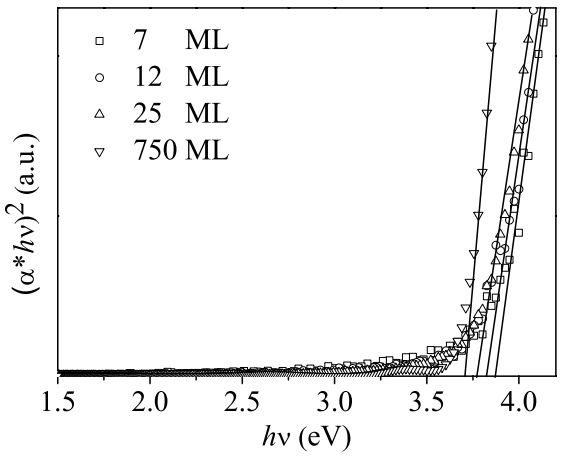

Fig. 4 – Absorption coefficient *vs.* incident phonon energy near the energy gap.

of the tetragonal phase is found in films thicker than 7 ML. Our results suggest that the compressive stress exists in films with different thicknesses and has a great effect on the band gap energy and Raman peaks shifts. The thinner the film is, the more the properties of the films deviate from those observed in bulk materials.

* * *

The authors would like to thank XIAOLONG LI for his help in XRD measurements and YULONG LIU for his help in Raman scattering measurements and many fruitful discussions. This work was supported by the key program for basic research of China.

REFERENCES

[1] SAYER M. and SREENIVAS K., *Science*, **247** (1990) 1065.
[2] COHEN R. E., *Nature (London)*, **358** (1992) 136.
[3] NAIR J. P., STAVITSKI N., GARTBMAN K., LUBOMIRSKY I. and ROYTBURD A. L., *Europhys. Lett.*, **60** (2002) 782.
[4] LEE M. B., KAWASAKI M, YOSHIMOTO M. and KOINUMA H., *Appl. Phys. Lett.*, **66** (1995) 1331.
[5] GARINO T. J. and HARRINGTON M., *Mater. Res. Soc. Symp. Proc.*, **243** (1992) 341.
[6] DESU S. B., *Phys. Status Solidi A*, **141** (1994) 119.
[7] TENNE D. A., XI X. X., LI Y. L., CHEN L. Q., SOUKIASSIAN A., ZHU M. H., JAMES A. R., LETTIERI J., SCHLOM D. G., TIAN W. and PAN X. Q., *Phys. Rev. B*, **69** (2004) 174101.
[8] ZHU J. S., LU X. M., JIANG W., TIAN W., ZHU M., ZHANG M. S., CHEN X. B., LIU X. and WANG Y. N., *J. Appl. Phys.*, **81** (1997) 1392.
[9] GIBERT S. G., WILLS L. A., WESSELS B. W., SCHINDLER J. L., THOMAS J. A. and KANNEWURF C. R., *J. Appl. Phys.*, **80** (1996) 969.
[10] LI A., GE C. Z. LU P., WU D., XIONG S. B. and MING N. B., *Appl. Phys. Lett.*, **70** (1997) 1616.
[11] ZHAO T., CHEN F., LU H. B., YANG G. Z. and CHEN Z. H., *J. Appl. Phys.*, **87** (2000) 7442.
[12] LOUDON R., *Adv. Phys.*, **60** (1964) 1025.
[13] GROENEN J., LANDA G., PIZANI P. S. and GENDRY M., *J. Appl. Phys.*, **82** (1997) 803.
[14] FONG D. D., STEPHENSON G. B., STREIFFER S. K., EASTMAN J. A., AUCIELLO O., FUOSS P. H. and THOMPSON C., *Science*, **304** (2004) 1650.
[15] FUNQUERA J. and GHOSEZ P., *Nature*, **422** (2003) 506.
[16] STREIFFER S. K., EASTMAN J. A., FONG D. D., THOMPSON C., MUNKHOLM A., MURTY M. V., AUCIELLO O., BAI G. R. and STEPHENSON G. B., *Phys. Rev. Lett.*, **89** (2002) 067601.
[17] YONEDA Y., OKABE T., SAKAUE K. and TERAUCHI H., *Surf. Sci.*, **410** (1999) 62.
[18] GUO H. Z., CHEN Z. H., LIU L. F., DING S., ZHOU Y. L., LU H. B., JIN K. J. and CHENG B. L., *Appl. Phys. Lett.*, **85** (2004) 3172.
[19] FREIRE J. D. and KATIYAR R. S., *Phys. Rev. B*, **37** (1988) 2074.
[20] SANJARJO J. A., KATIYAR R. S. and PORTO S. P. S., *Phys. Rev. B*, **22** (1980) 2396.
[21] GUO H. Z., LIU L. F., DING S., LU H. B., ZHOU Y. L., CHENG B. L. and CHEN Z. H., *J. Appl. Phys.*, **96** (2004) 3404.
[22] YUZYUK Y. I., ALYOSHIN V. A., ZAKHARCHENKO I. N., SVIRIDOV E. V., ALMEIDA A. and CHAVES M. V., *Phys. Rev. B*, **65** (2002) 134107.
[23] HWANG C. S., *J. Appl. Phys.*, **92** (2002) 432.
[24] TAKAHURA K., HIROI N., SUEMASU T., CHICHIBU S. F. and HASEGAWA F., *Appl. Phys. Lett.*, **80** (2002) 556.